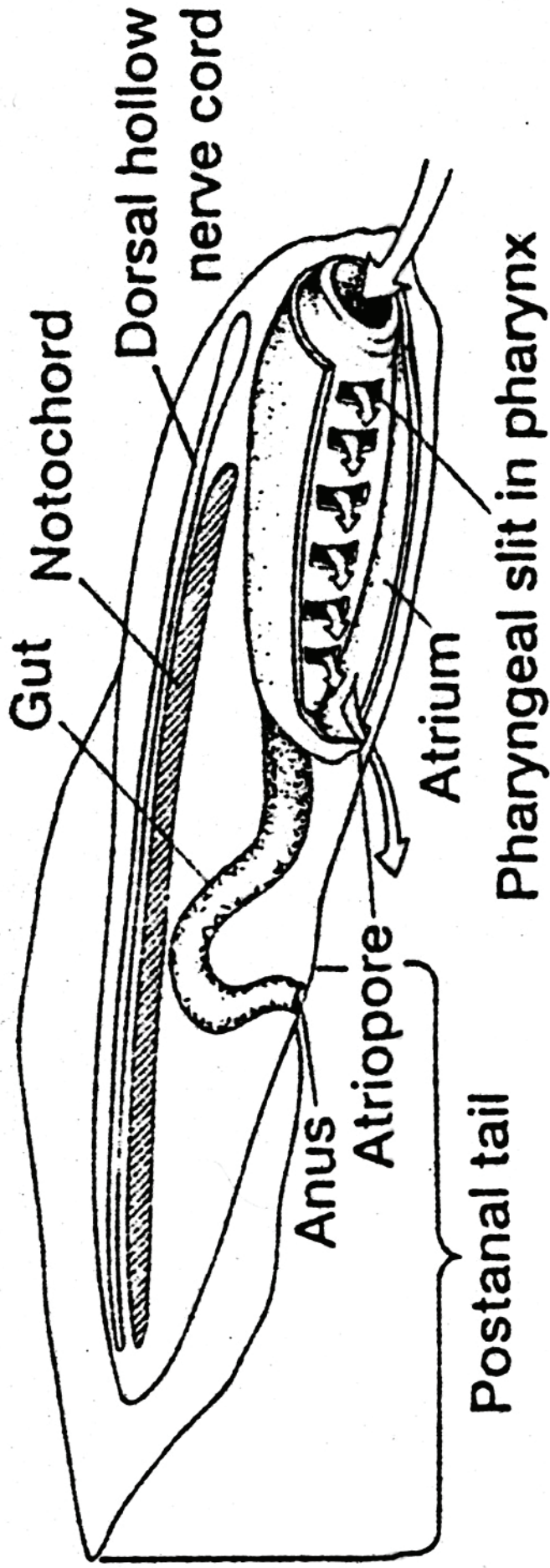
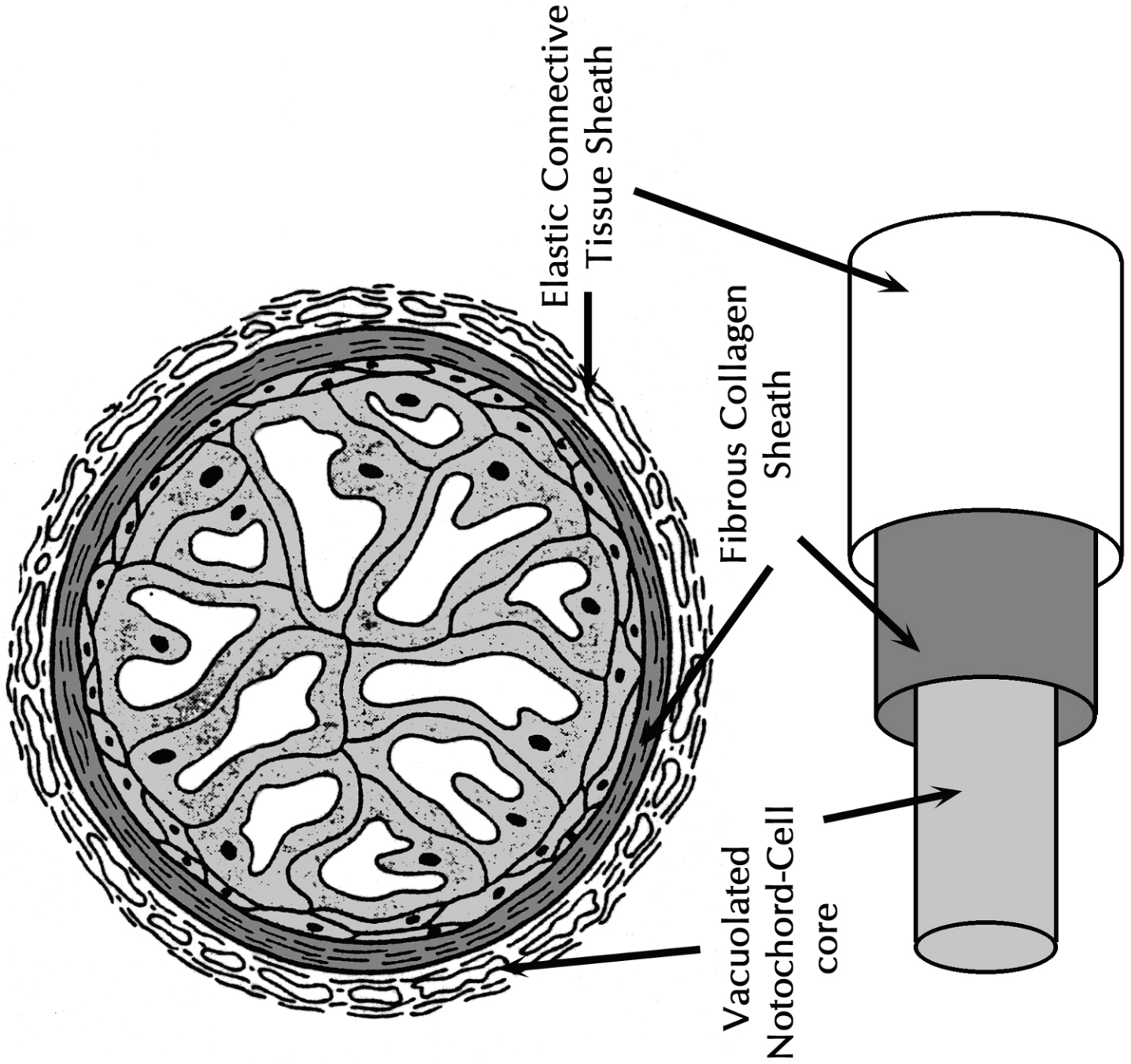
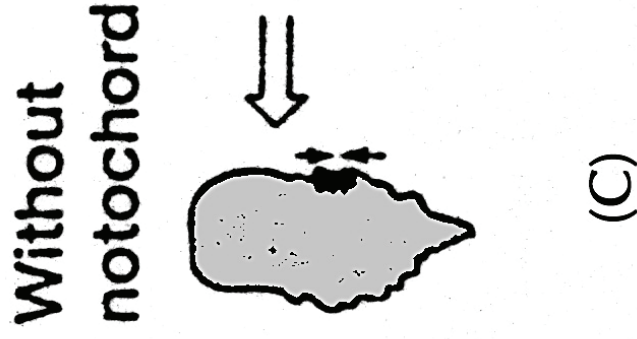
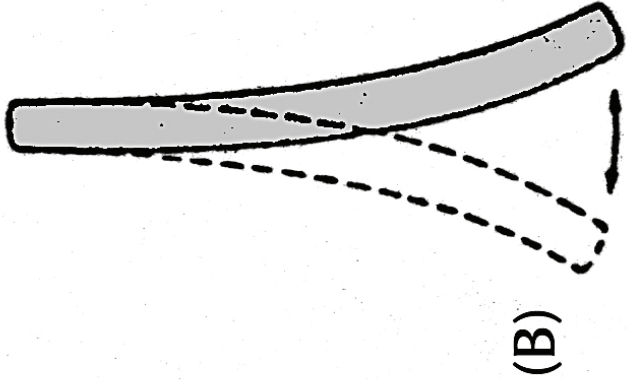
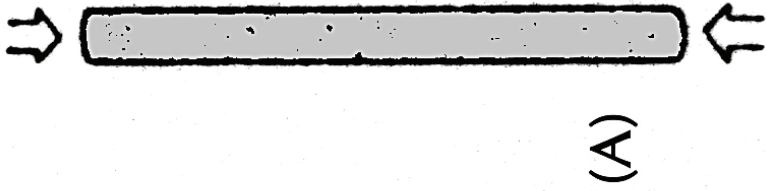


Comparative Anatomy & Evolution of Vertebrates





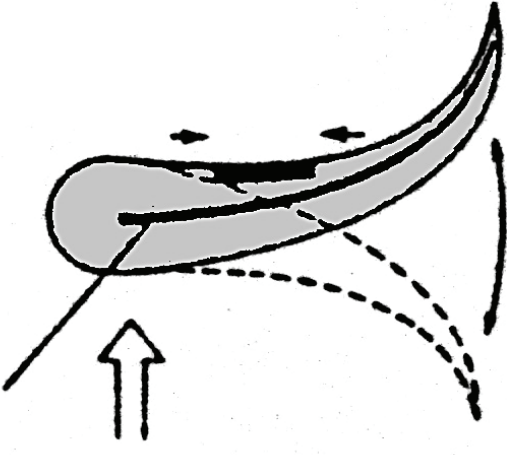


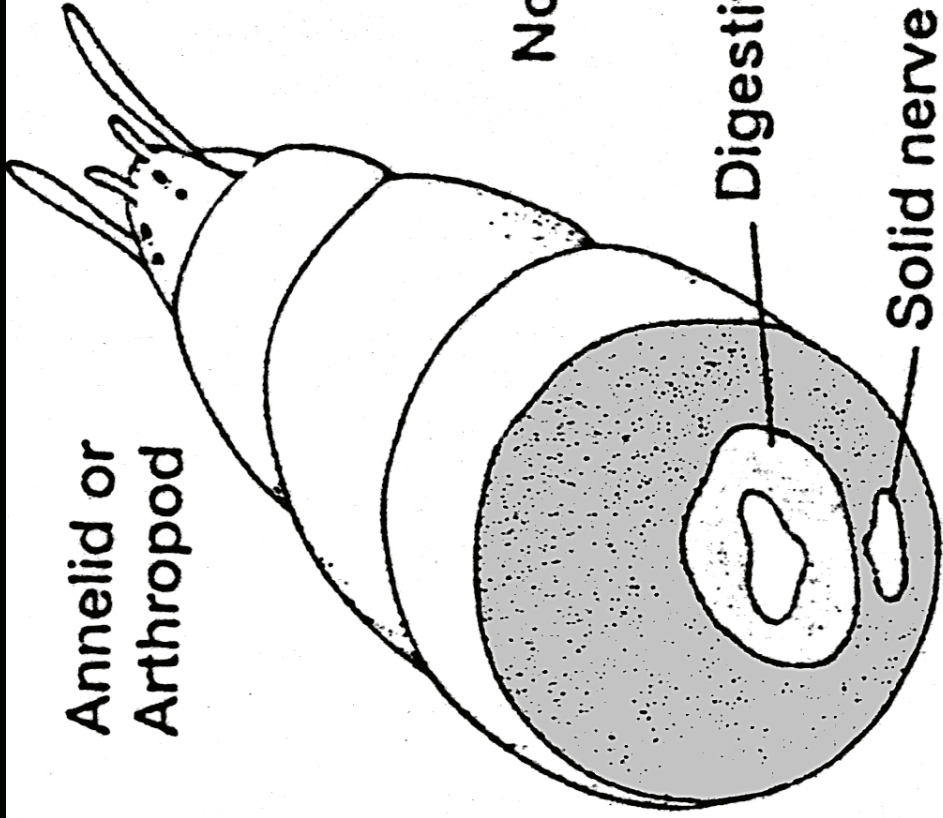


Without
notochord

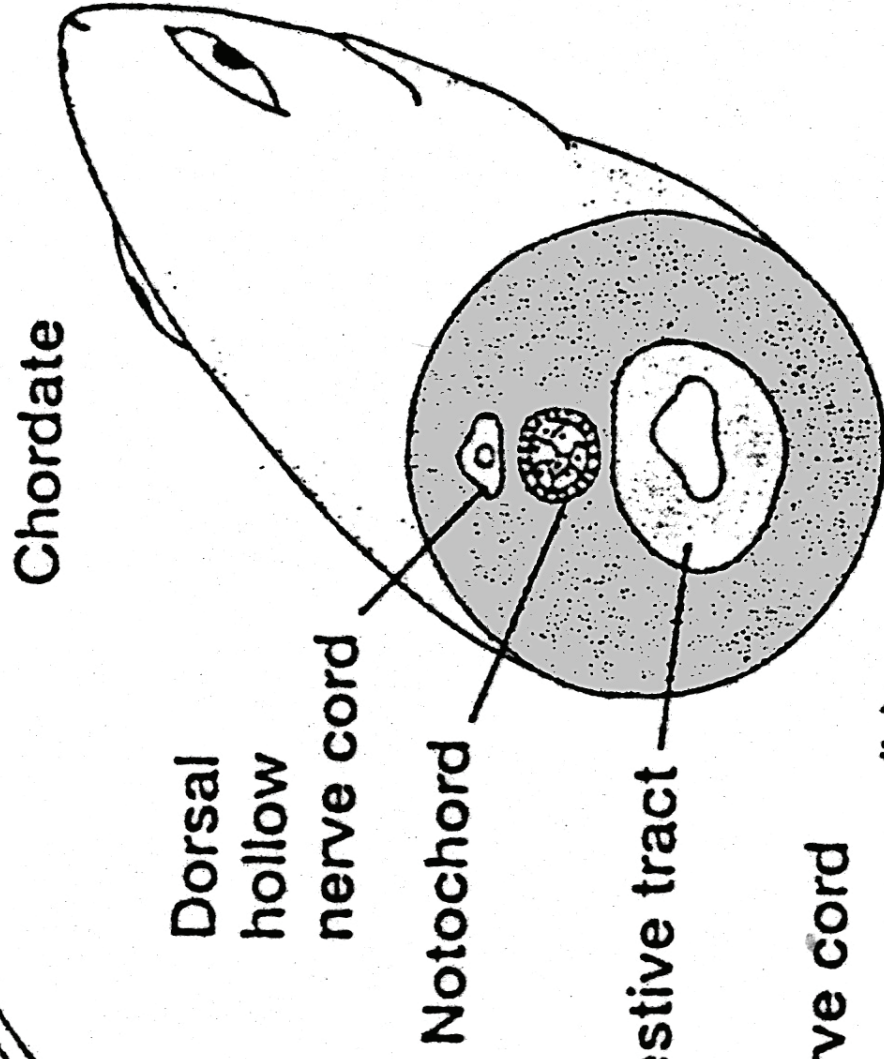


With
notochord





(a)



(b)

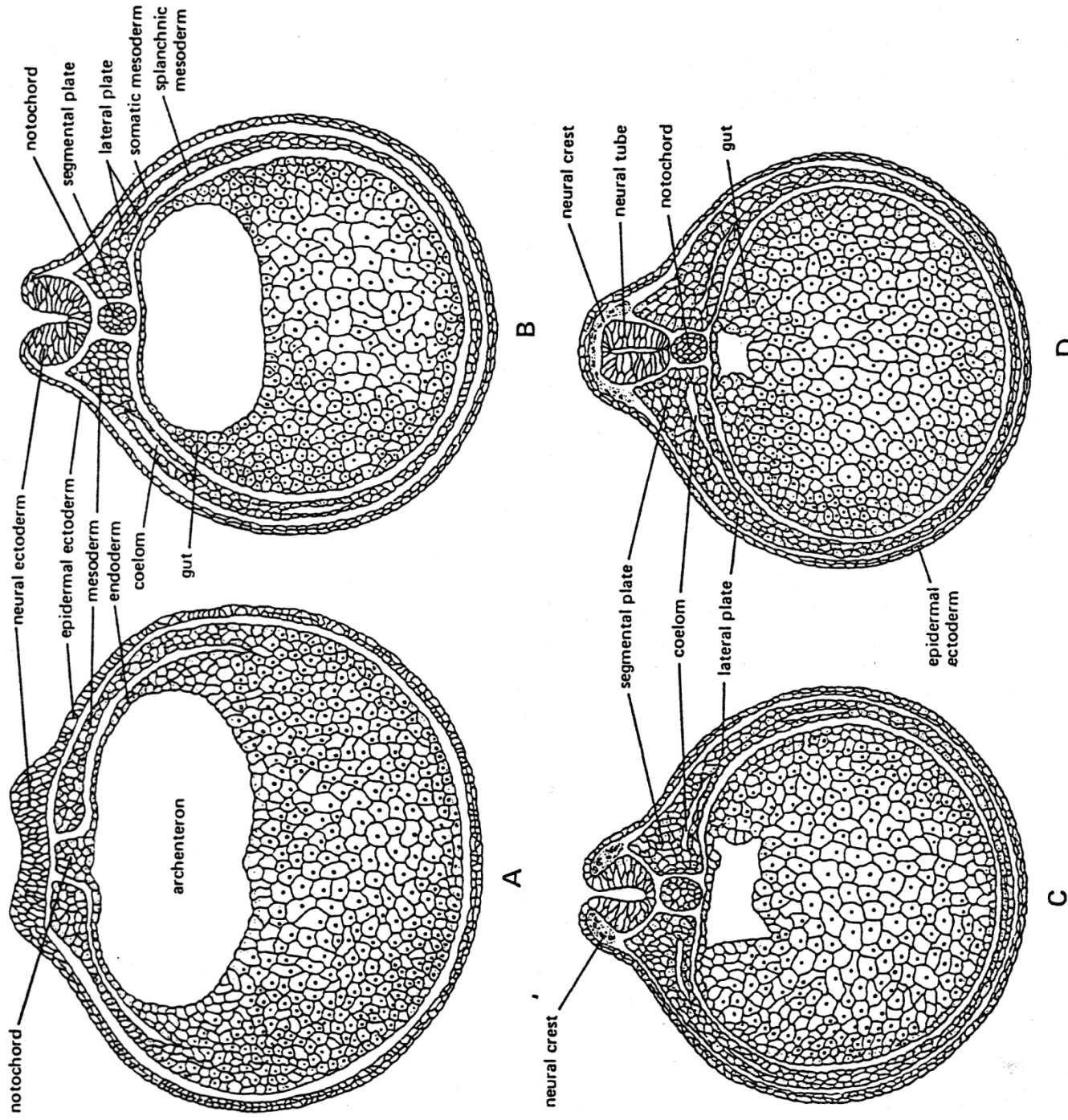


FIGURE 26. Successive developmental stages of a frog embryo. These semidiagrammatic cross sections follow the process of neural tube formation. (After Holmes, Huettner)

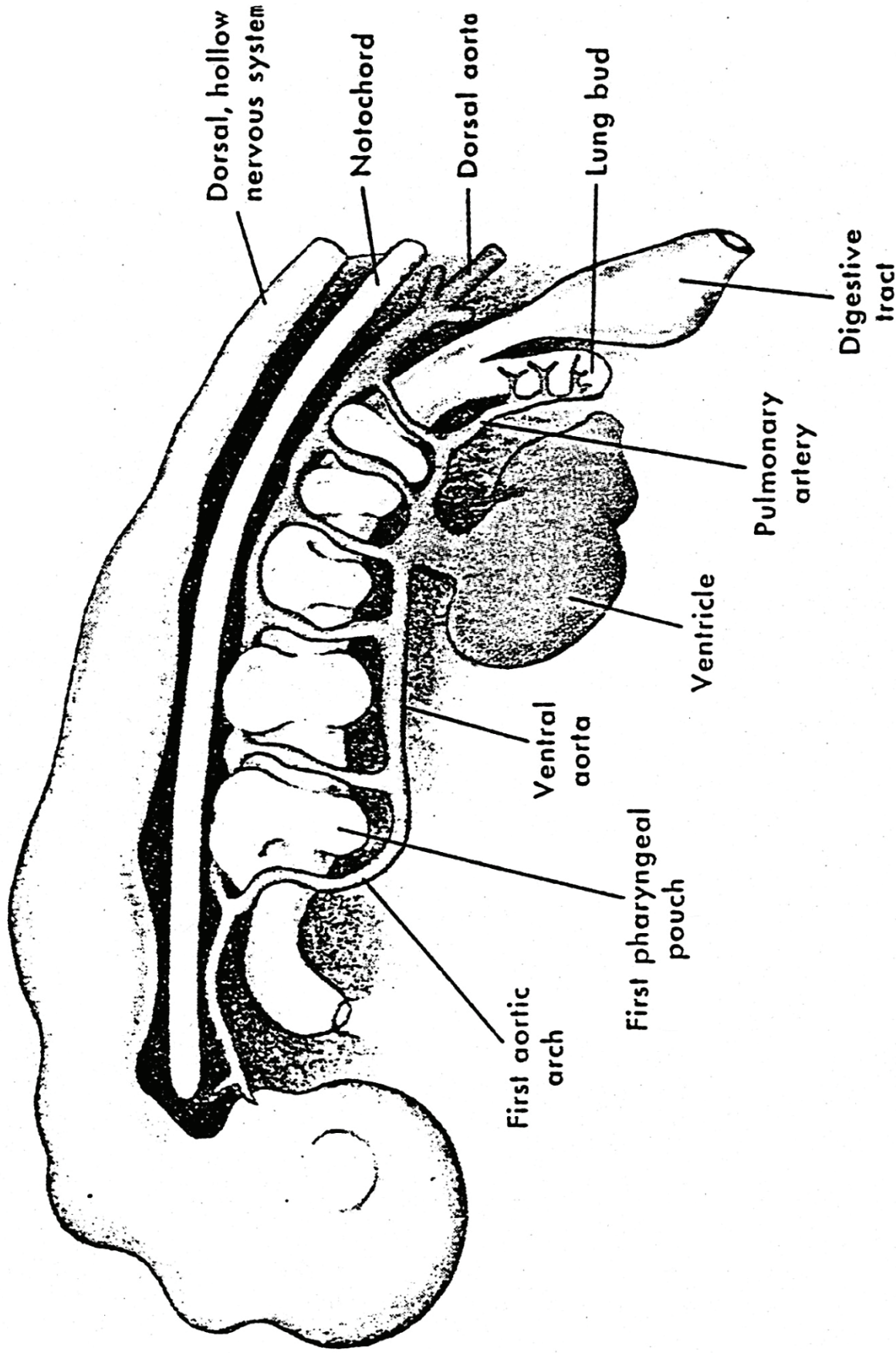


FIGURE 27. Basic pharyngeal architecture in a composite vertebrate embryo. The dorsal aorta is paired in the head but the ventral aorta is unpaired. A series of pharyngeal pouches has evaginated from the lateral walls of the digestive tract. Six aortic arches connect the heart and ventral aorta with the dorsal aorta. (The first aortic arch typically disappears before the 6th is formed.)

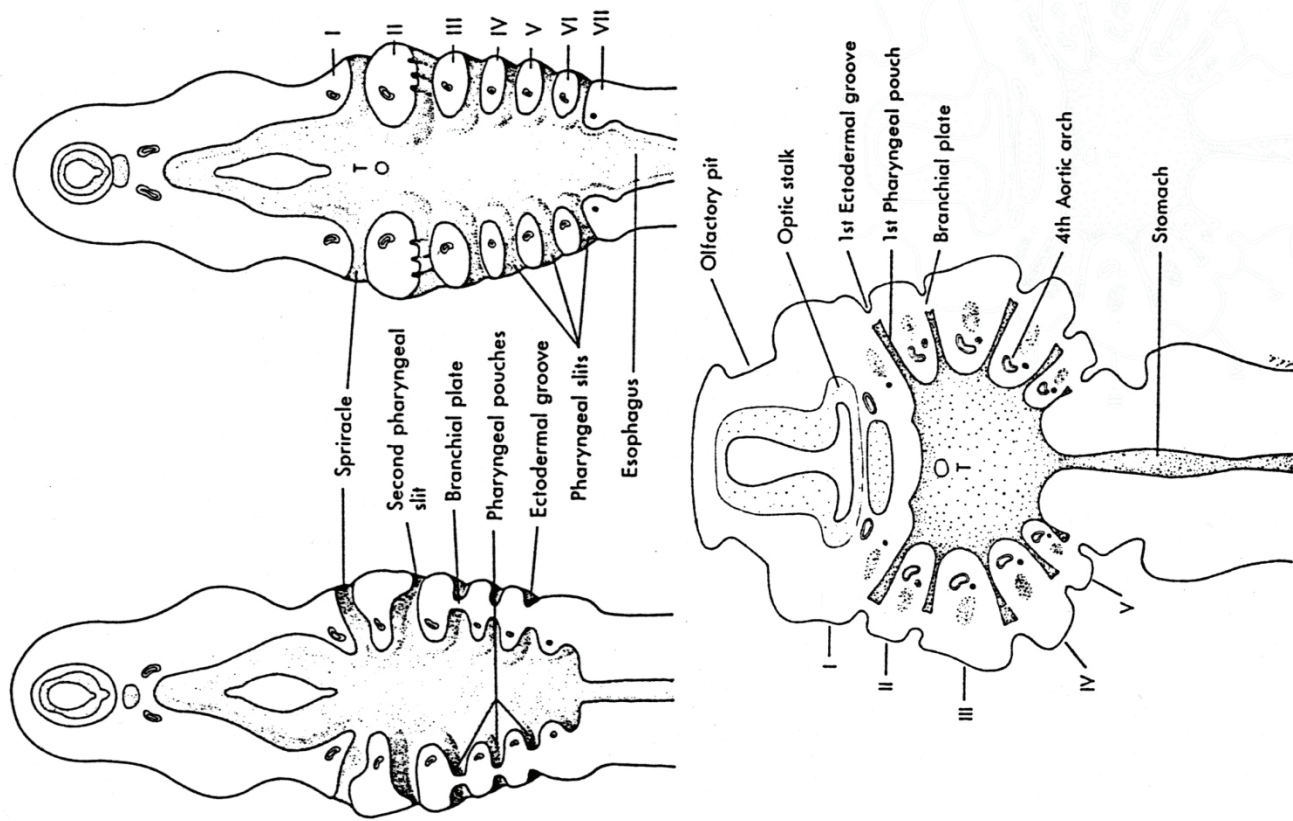


FIGURE 28. Frontal sections of pharyngeal regions in an embryonic shark (early, top left; late, top right) and frog (bottom). Roman I - VII mark the pharyngeal pouches surrounding the pharyngeal pouches, clefts and/or slits. T marks the evagination of the thyroid.

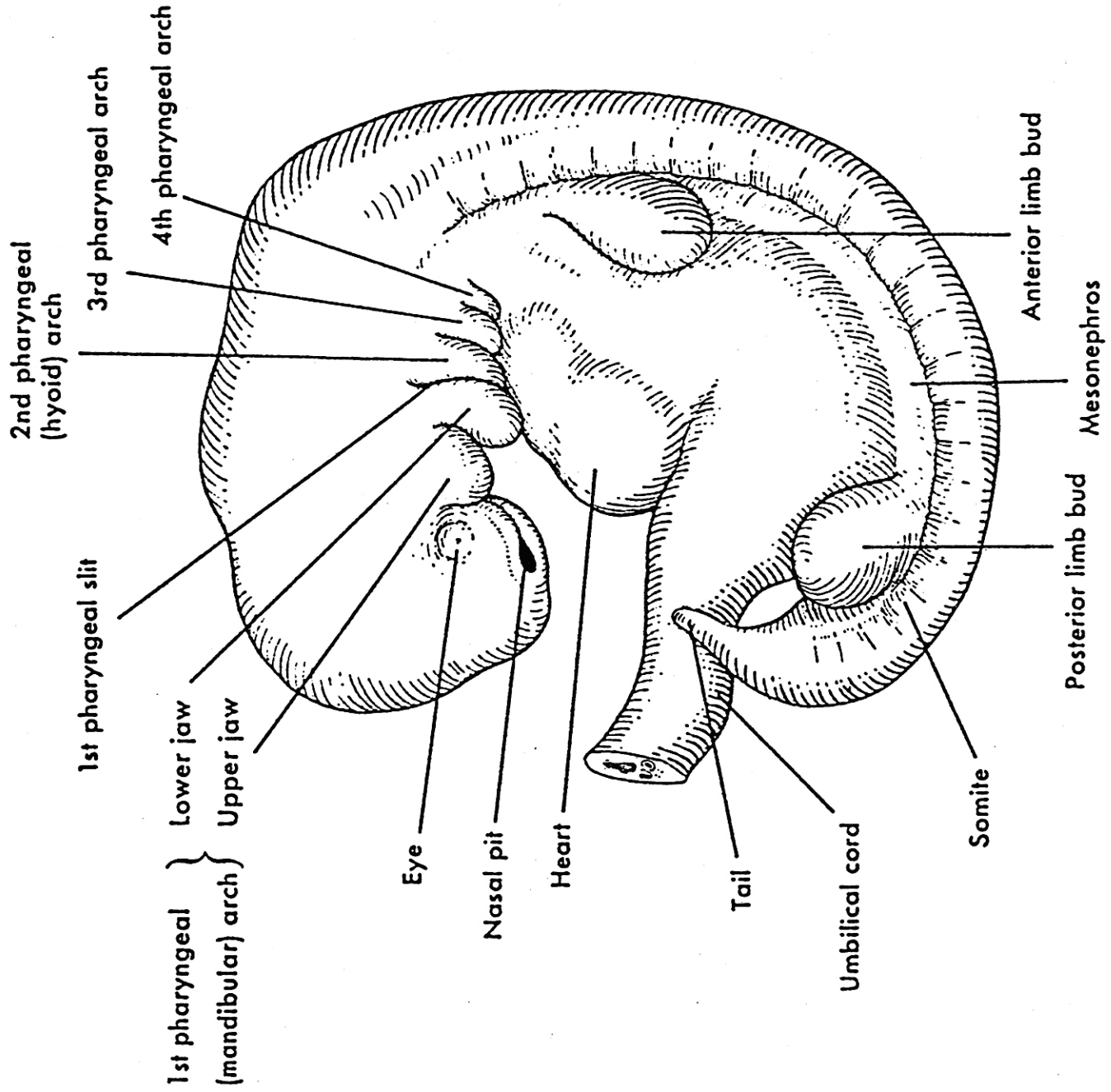


FIGURE 29. Human embryo approximately 4/12 weeks after fertilization (5-mm stage).

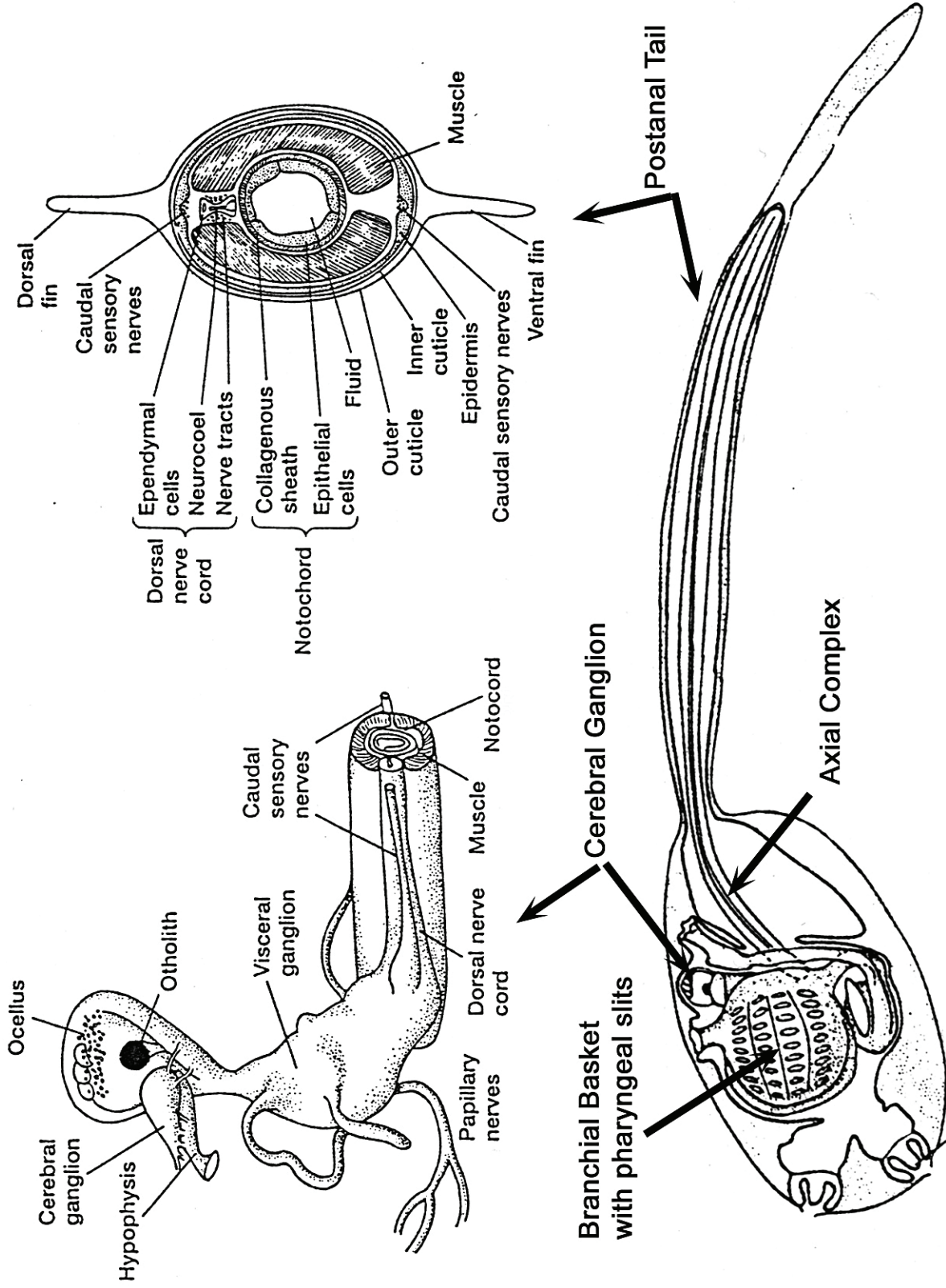


FIGURE 30. Structural Anatomy of the subphylum Urochordata, class Ascidiacea, *Distaplia occidentalis*. Larval form demonstrating basic chordate hallmarks (bottom). Detail of cerebral ganglion and structural relationship to the axial complex (upper left). Cross-sectional anatomy of postanal tail and axial complex (upper right).

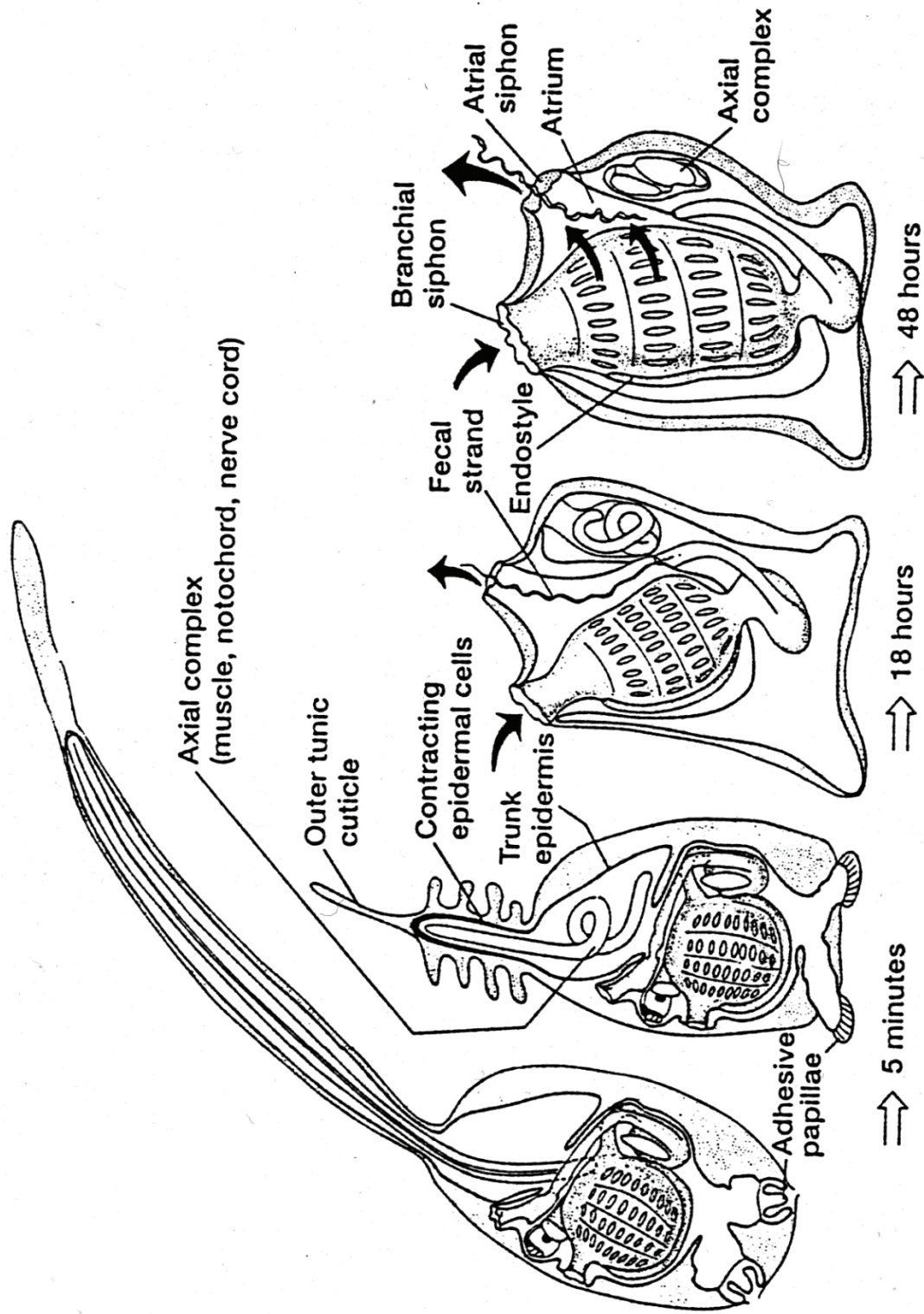
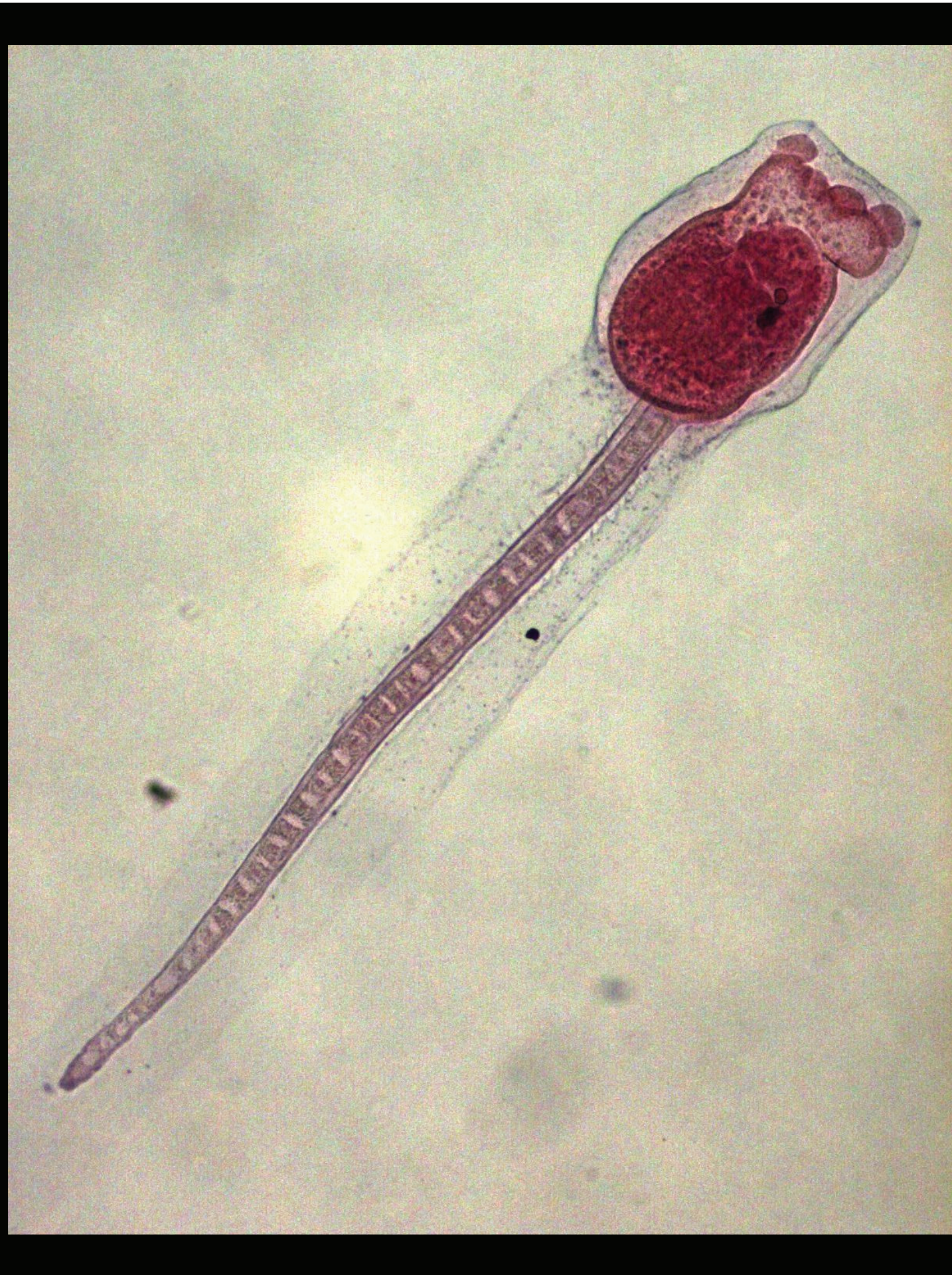
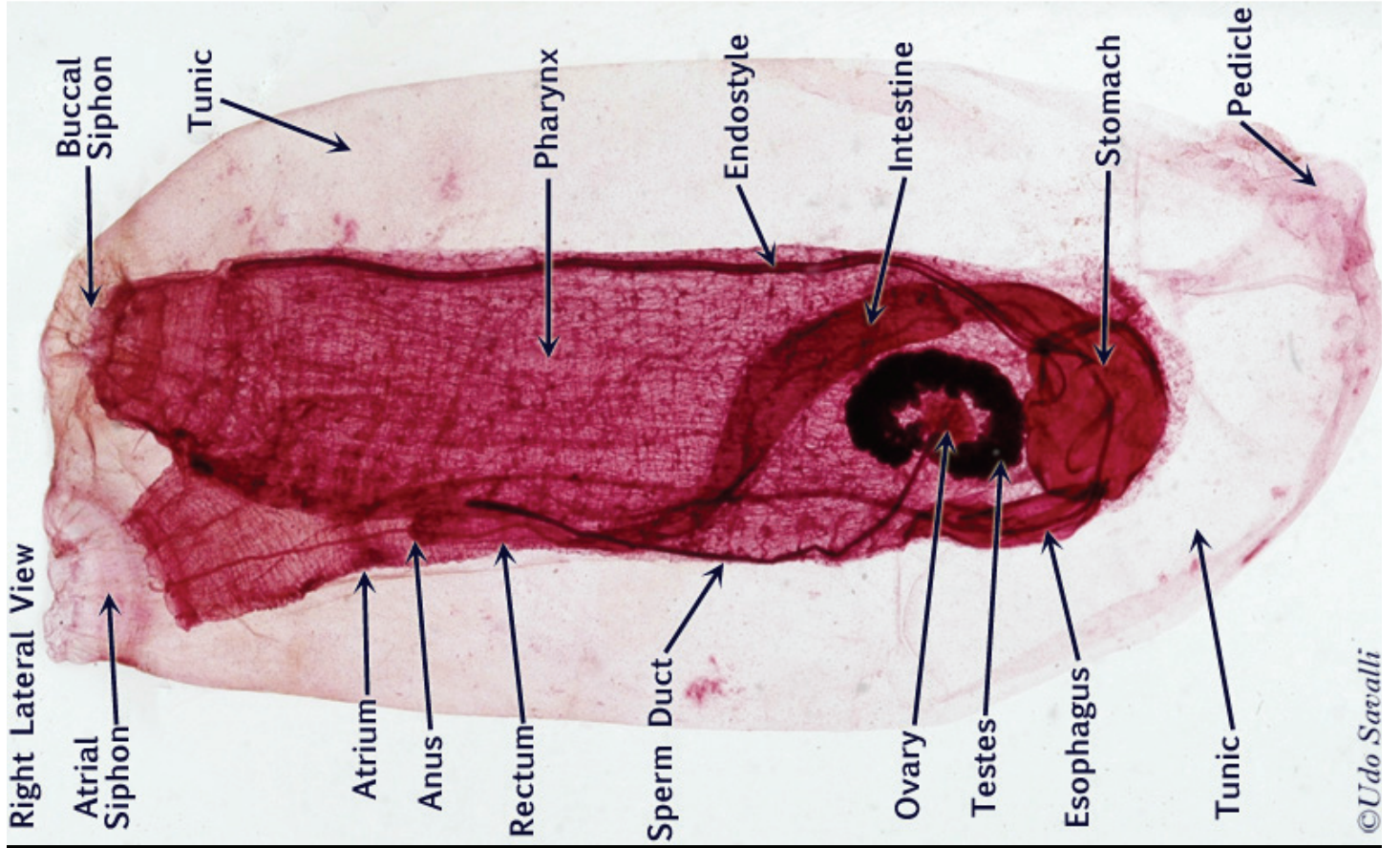
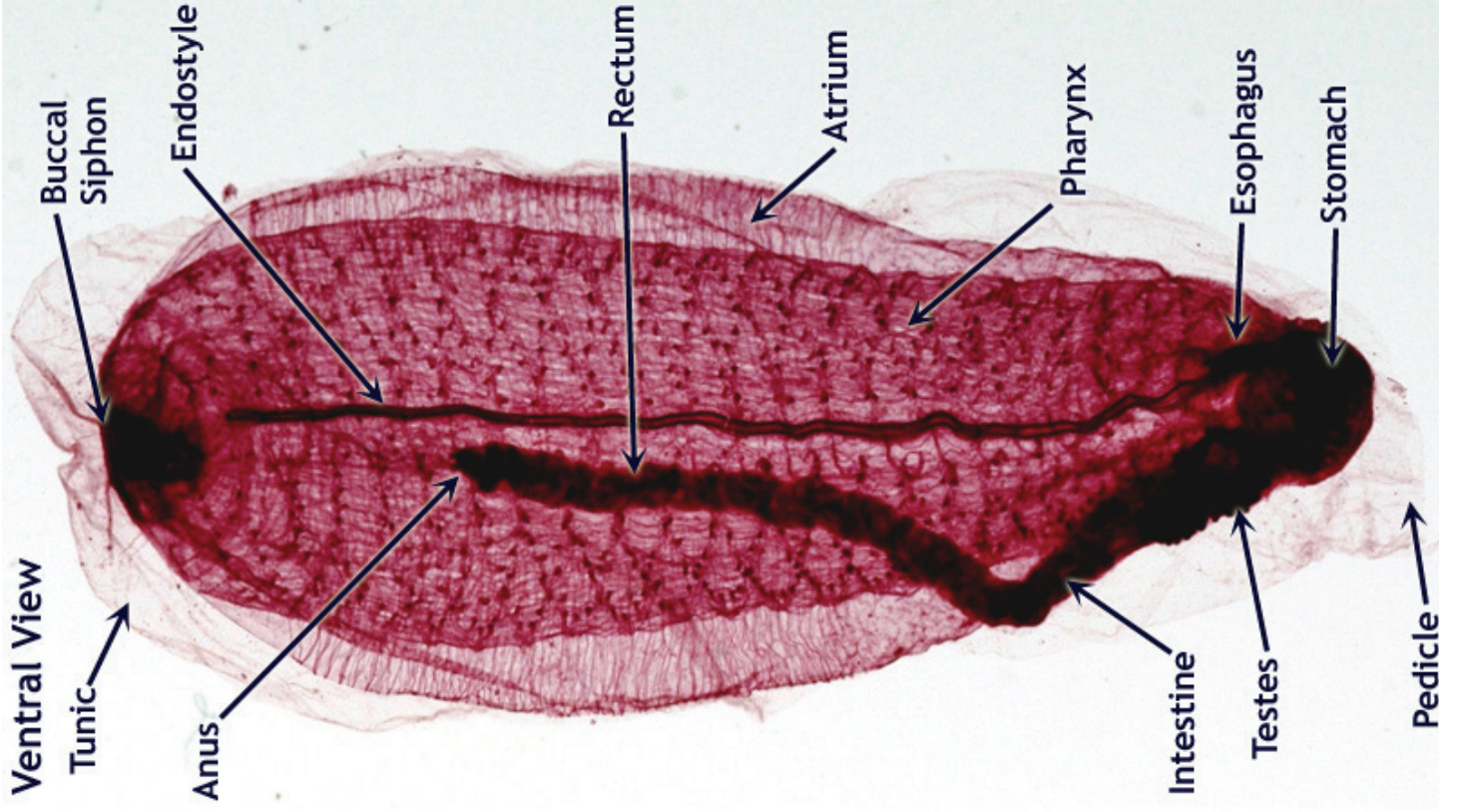


FIGURE 31. Metamorphosis of the ascidian larva *Distaplia*. The planktonic non-feeding larva settles and attaches to the substrate. Adhesive papillae hold the larva in place. Contraction of the tail epidermis pulls the axial complex into the body and the larva sheds its outer cuticle following attachment. By 18 hours the branchial basket rotates to reposition the siphons and active feeding has begun as evidenced by the presence of a fecal strand. By 48 hours most of axial complex is resorbed, rotation is complete, and attachment to the substrate is firm. (R A Cloney)





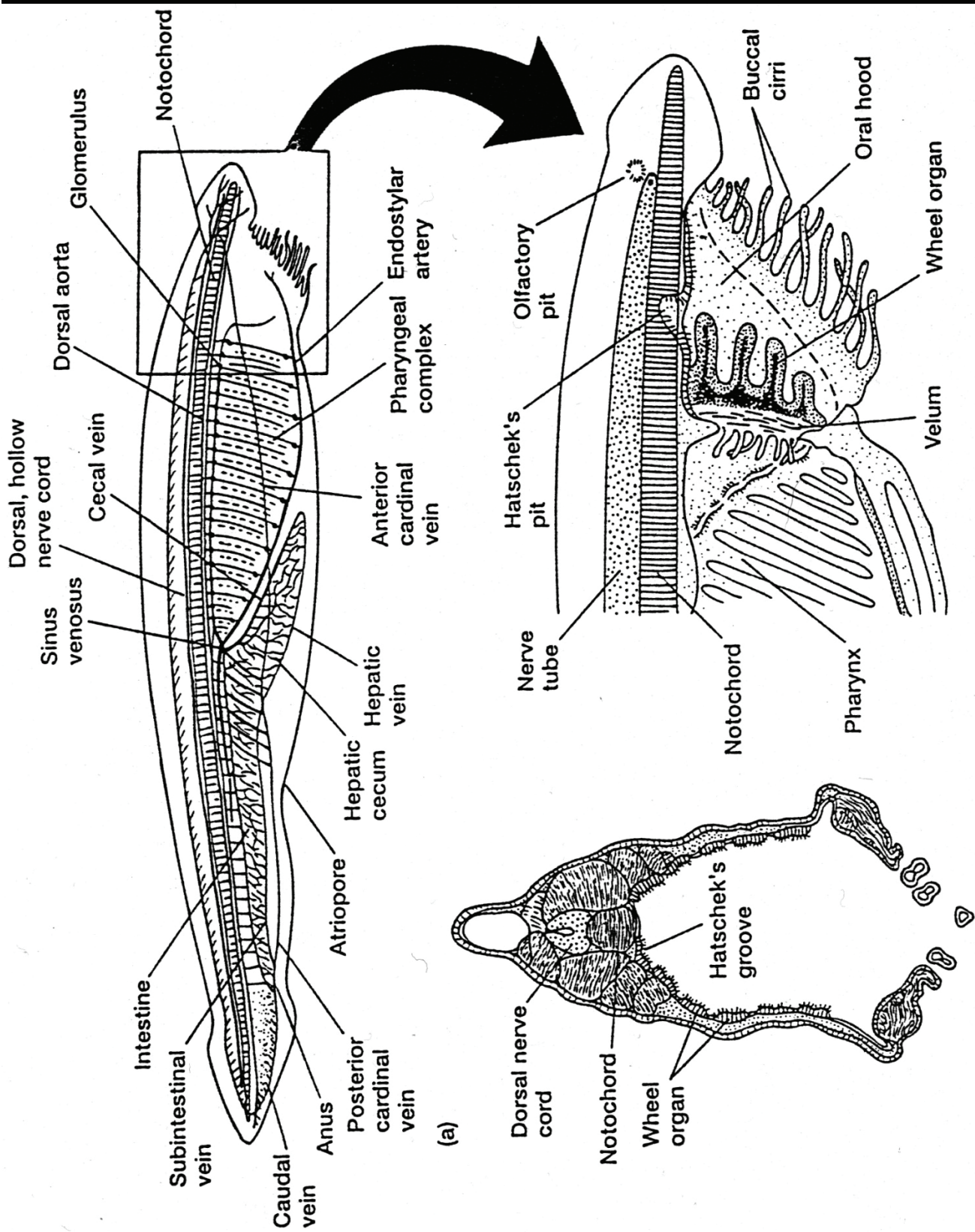


FIGURE 32. Structural anatomy of the subphylum Cephalochordata, *Branchiostoma lanceolatum*. (a) Lateral view. (b) Cross section through oral hood. (c) Mouth area.



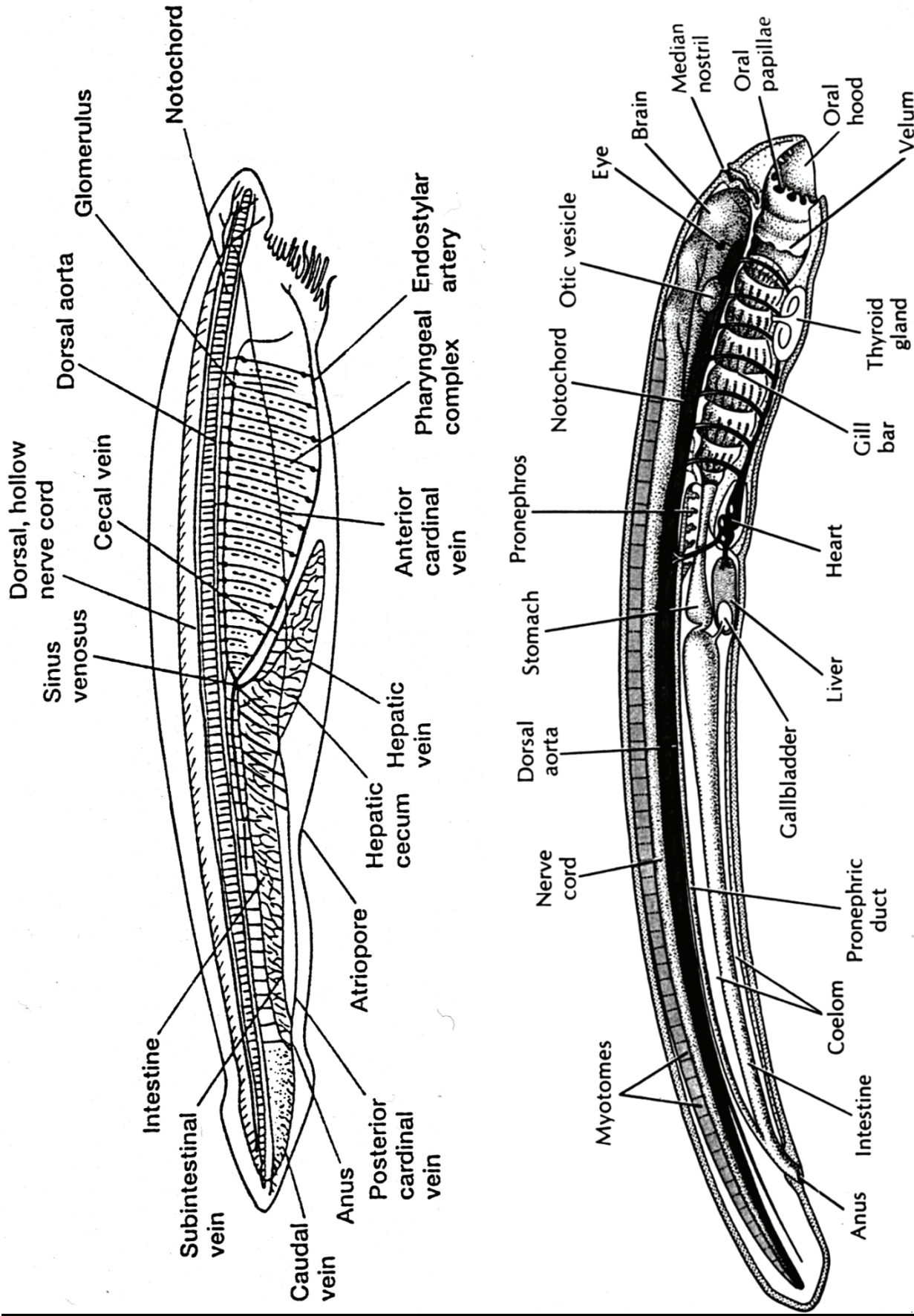


FIGURE 33. Comparative anatomy of the cephalochordate *Branchiostoma* (top) and the ammocete larva of a lamprey (Bottom). Although these forms bear a striking general resemblance the ammocete has a well-developed brain rather than a cerebral ganglion. The ammocete also has median eyes, a pronephretic kidney and other features lacking in amphioxus.

©Udo M. Savalli



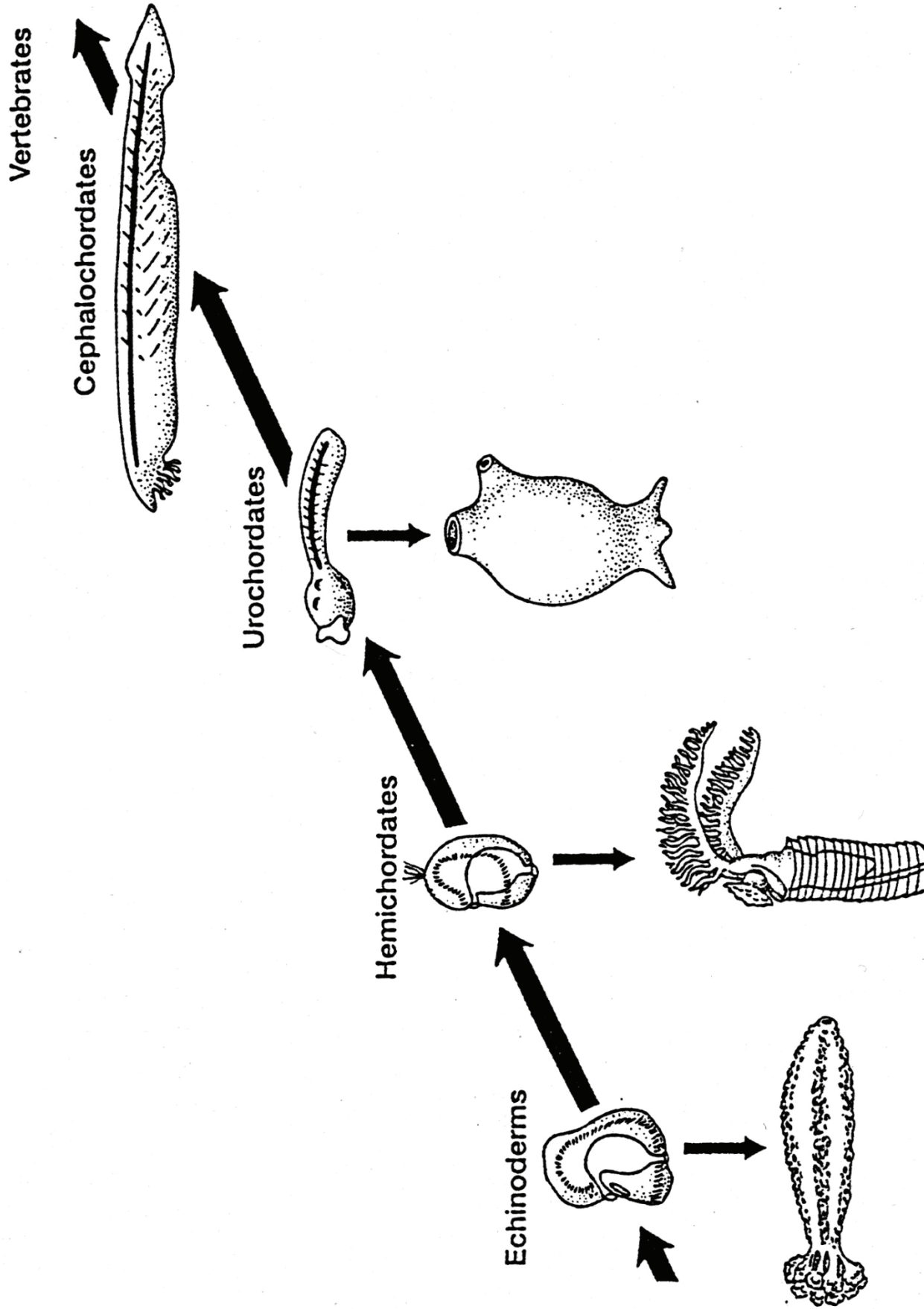
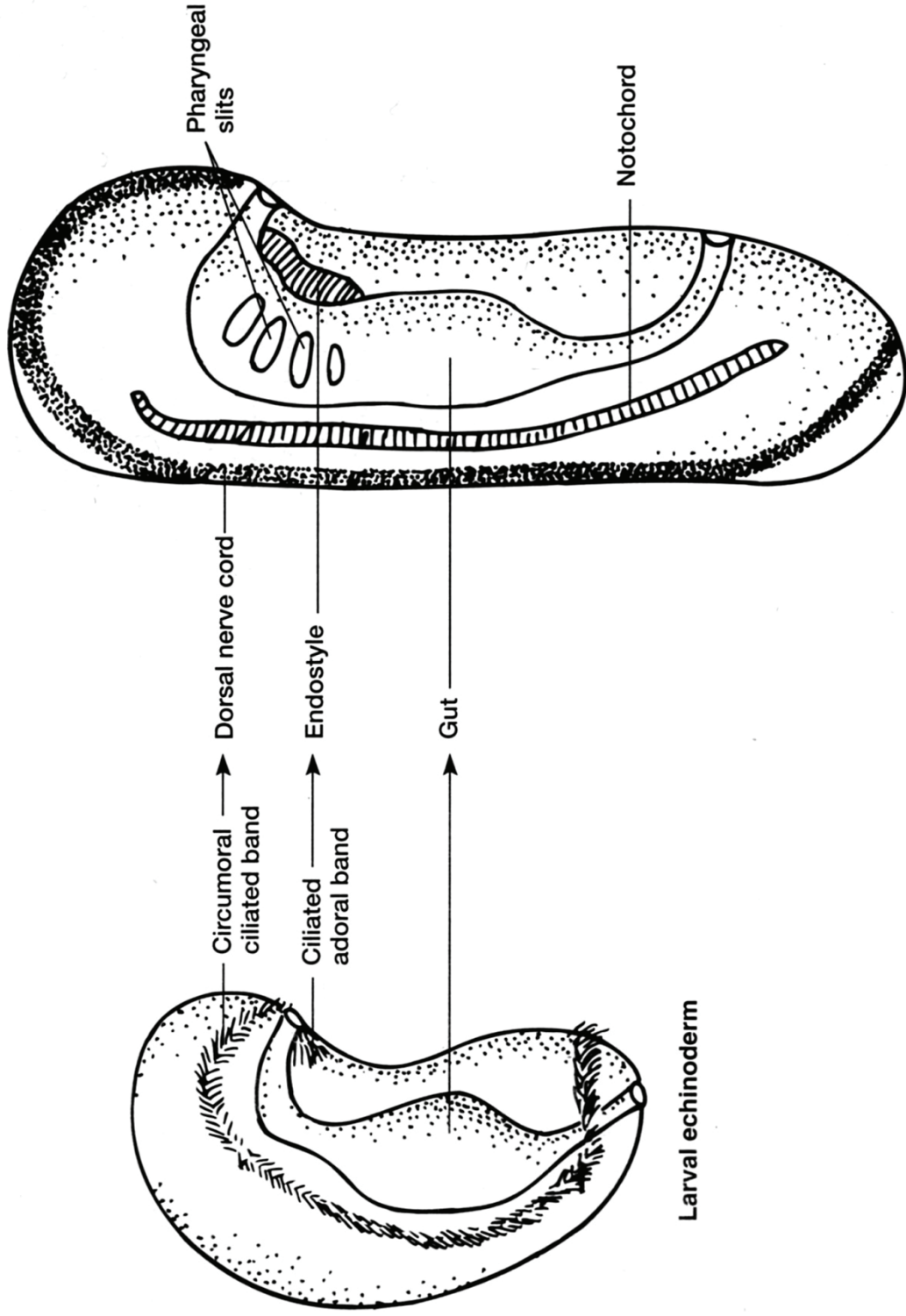


FIGURE 34. Summary of Garstang's Hypothesis of Chordate Heterochrony (The Paedomorphic Hypothesis). Garstang proposed a series of literal evolutionary steps through larval stages, beginning with echinoderms and eventually producing chordates via heterochrony.



Chordate body plan

FIGURE 35. Hypothesis of Chordate Heterochrony: Echinoderms to protochordates. The proposed common ancestor of the protochordates (left) was bilaterally symmetrical and externally resembled an echinoderm auricularian larva. The ancestor's circumoral ciliated bands and their underlying nerve tracts moved dorsally, meeting and fusing to form the dorsal nerve cord. The adoral ciliated band gave rise to the endostyle and the pharyngeal ciliated tracts. The appearance of pharyngeal slits dramatically improves water-flow and feeding efficiency. The notochord is a locomotor advantage in the larger organism.

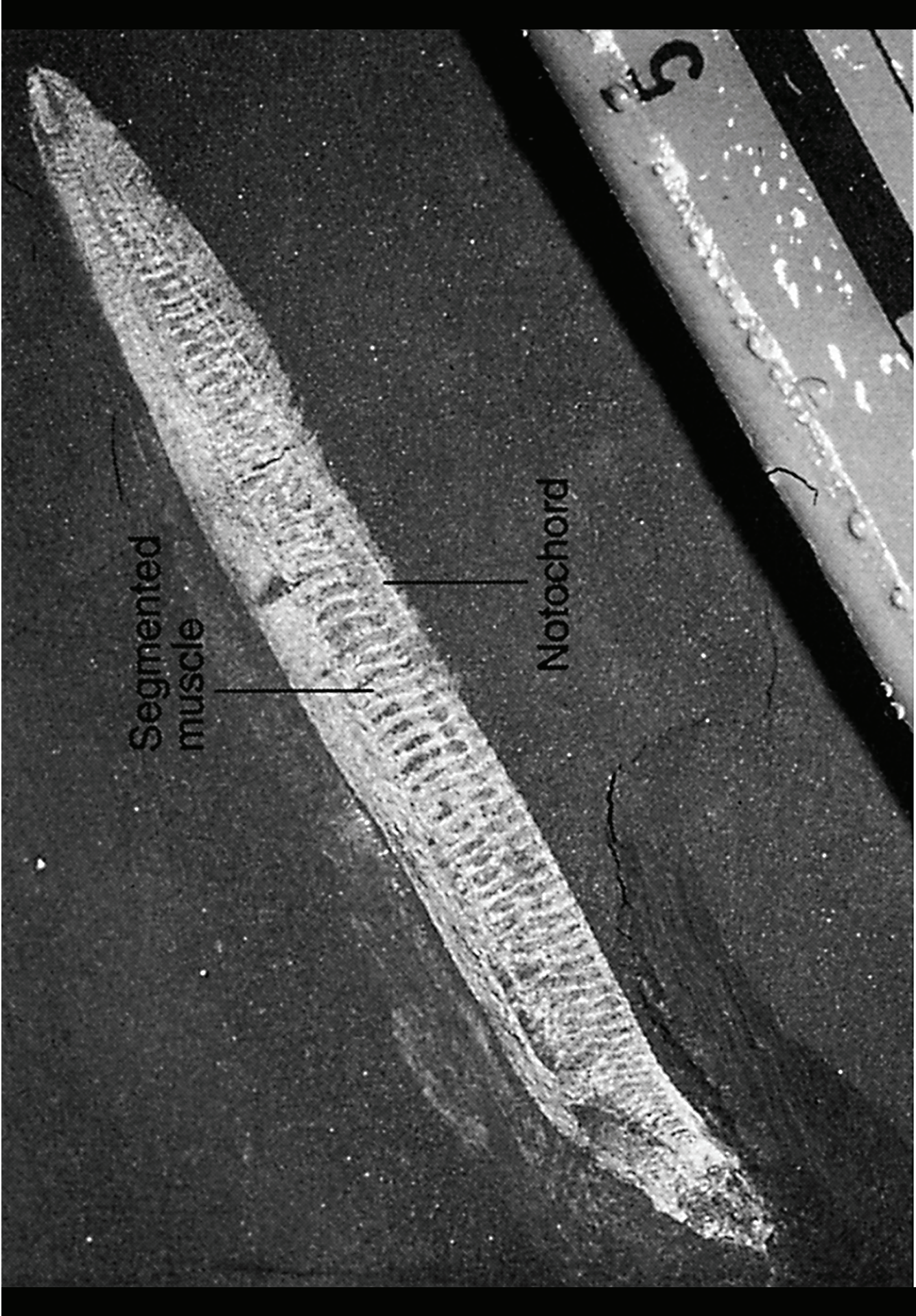


FIGURE 36. *Pikaia gracilis*, among the oldest known chordates. 520 million year old fossil recovered from the mid-Cambrian Burgess Shale Beds, British Columbia, Canada.



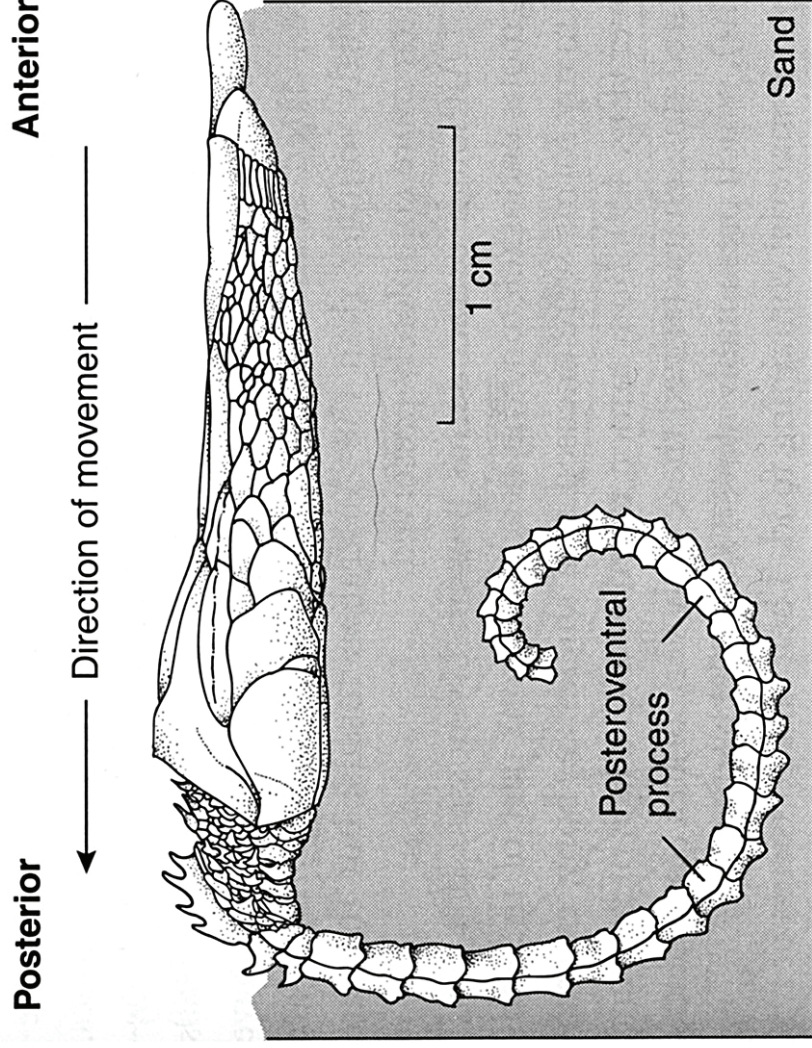
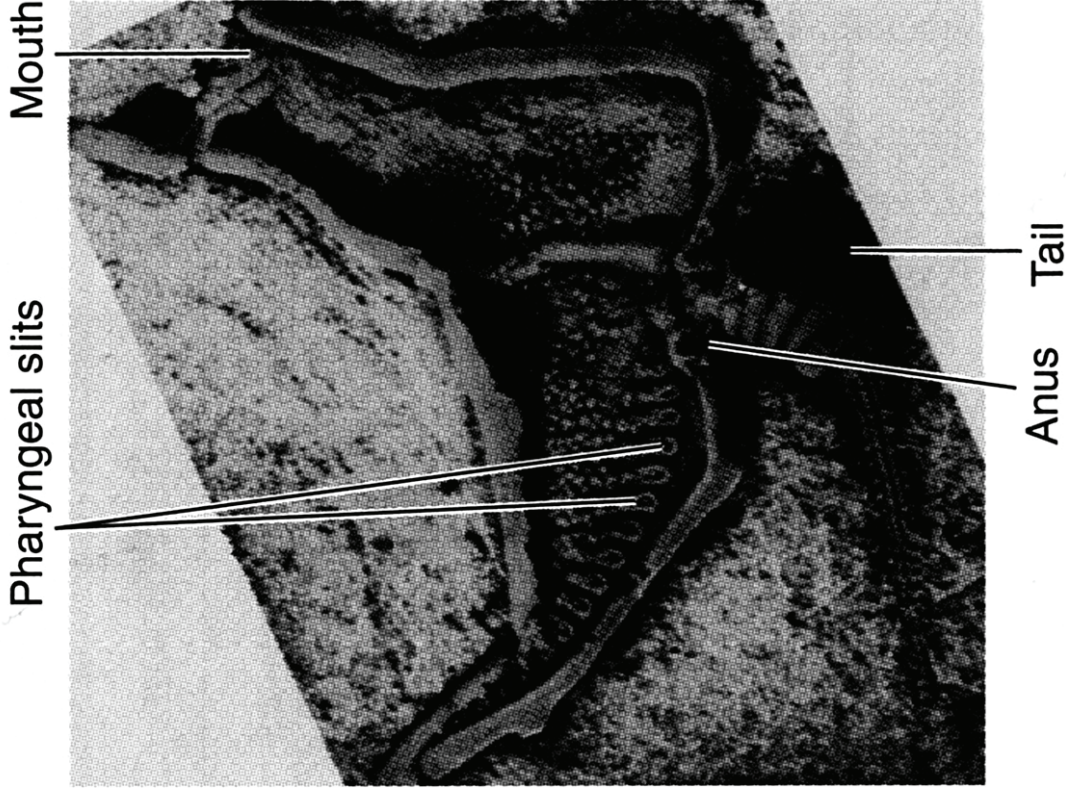


FIGURE 37. Calcichordates. Fossil of an early echinoderm calcichordate from Ordovician deposits (450 million years ago) (left). These animals show strong affinities with both chordates and echinoderms and may belong to an ancestral chordate lineage. Lateral habitus interpretation of a calcicochordate. Note the overlapping calcium carbonate plates covering the body (a distinct echinoderm feature). Also note that fossil interpretation is often at odds even within a single taxon.

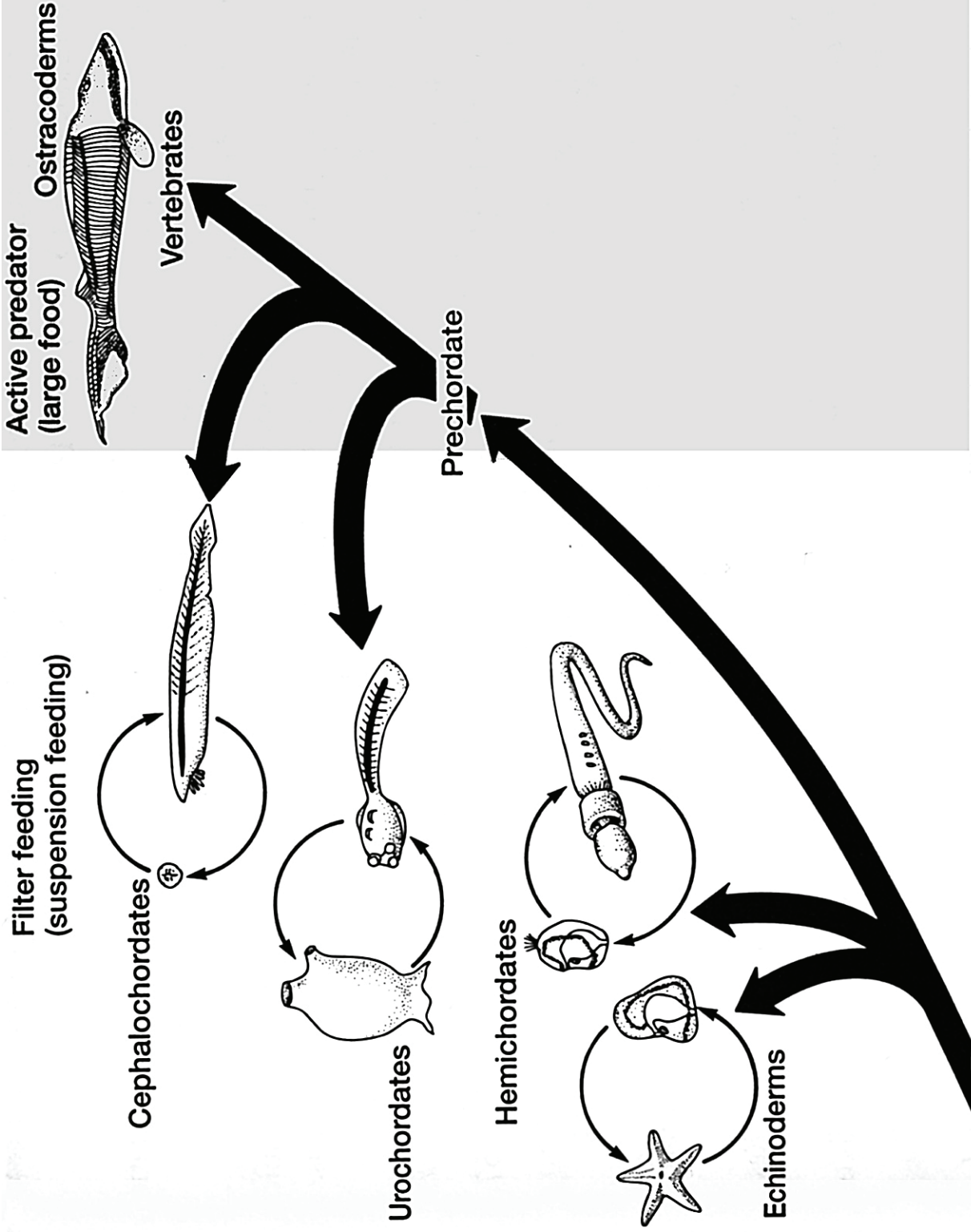


FIGURE 38. Diploleuloid Theory of Chordate Evolution. The tendency to abandon the sedentary lifestyle of filter feeding in favor of a more active predaceous life initially favored development of a prechordate with notochord, muscular tail, and dorsal tubular nerve cord. Continuation of this trend gave rise to vertebrates, but urochordates and cephalochordates reversed the trend and returned secondarily to suspension-feeding life styles and forms.

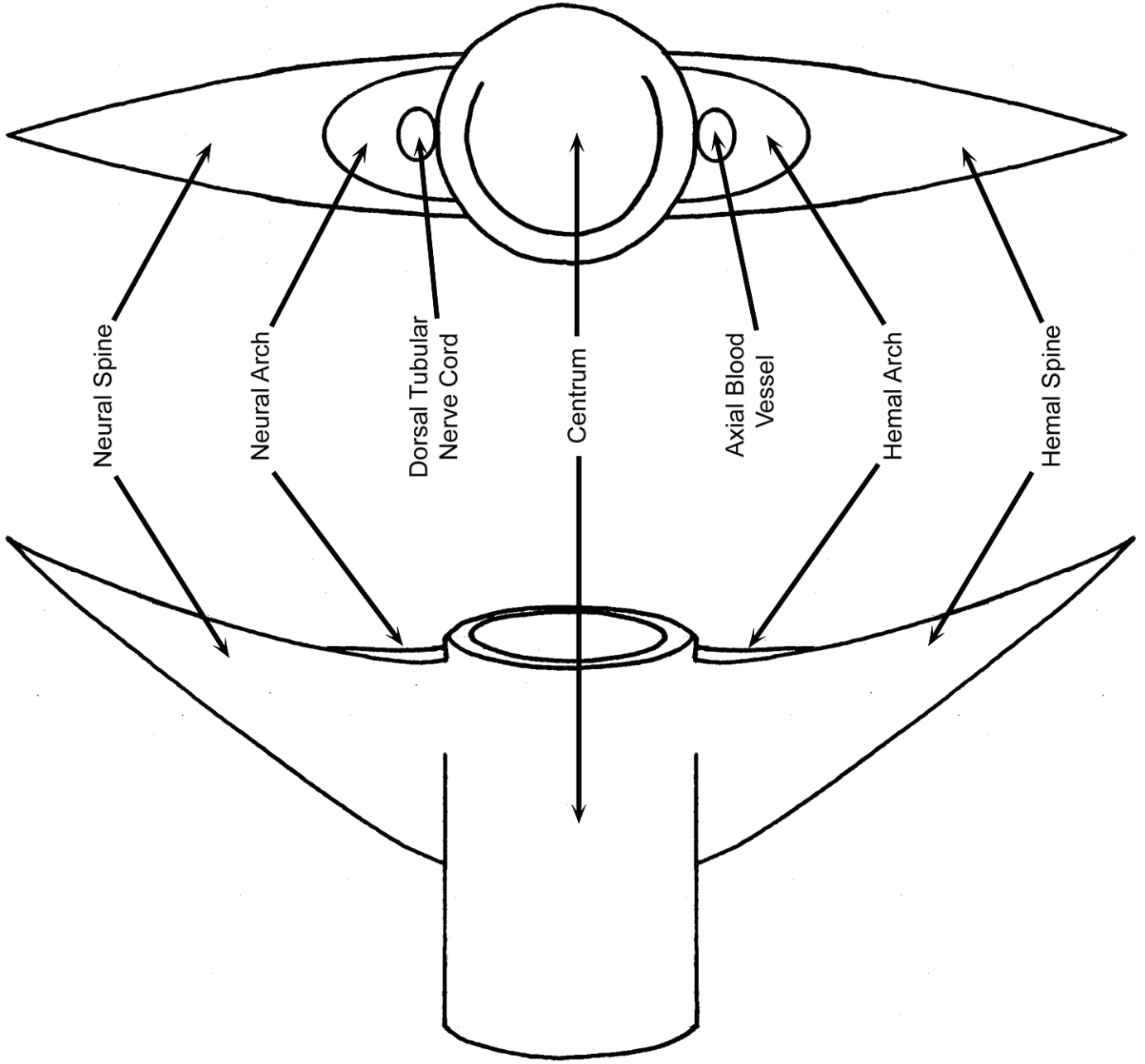


FIGURE 39. General structure of a holospondylic vertebra.

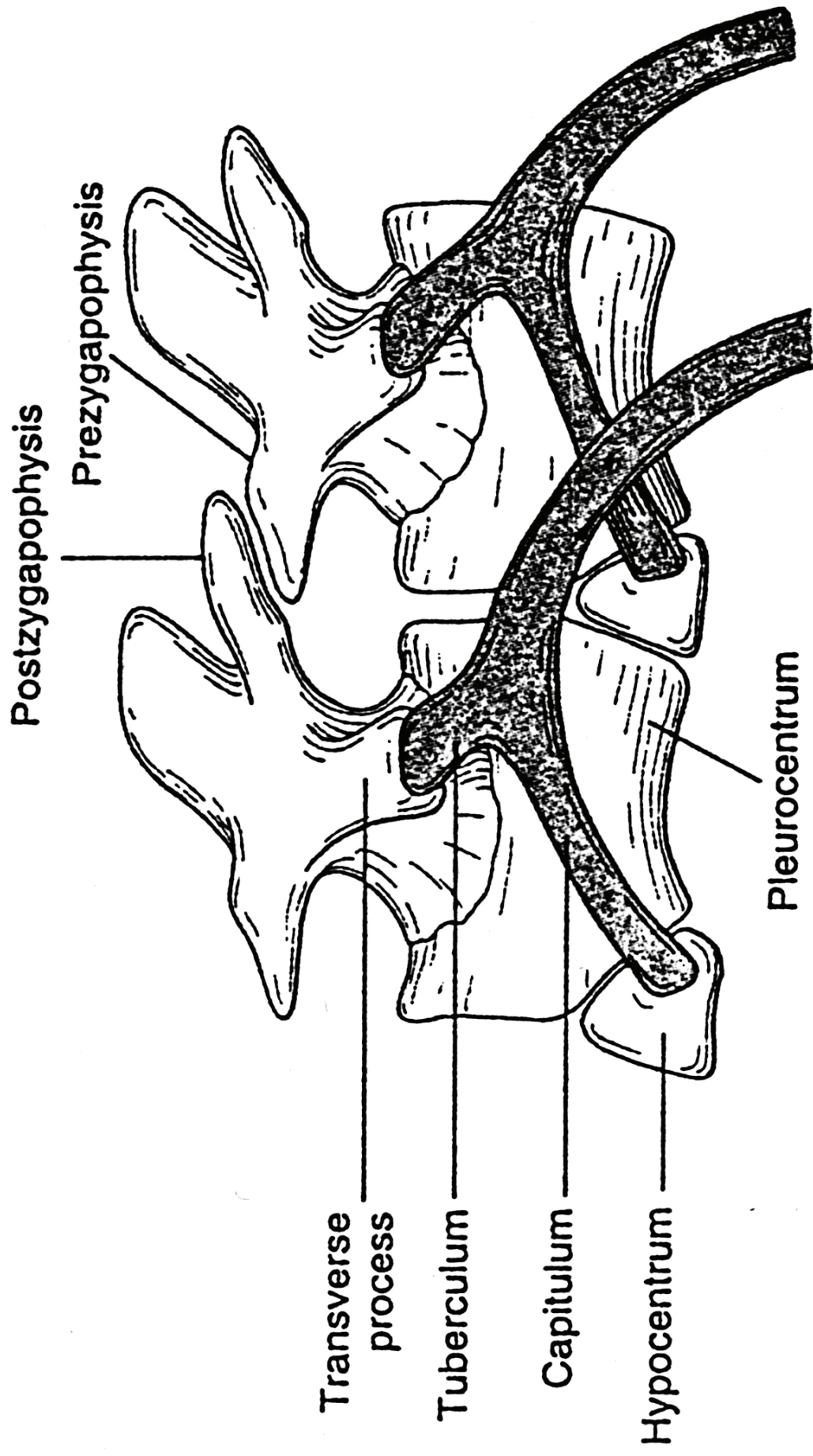


FIGURE 40. General structure of aspidospondylic vertebrae. The prezygapophysys of the trailing vertebra intercalate with the postzygapophysys of the lead vertebra to maintain alignment and limit dorso-ventral flexure. The transverse processes (diapophyses) provide points of articulation for the thoracic ribs.

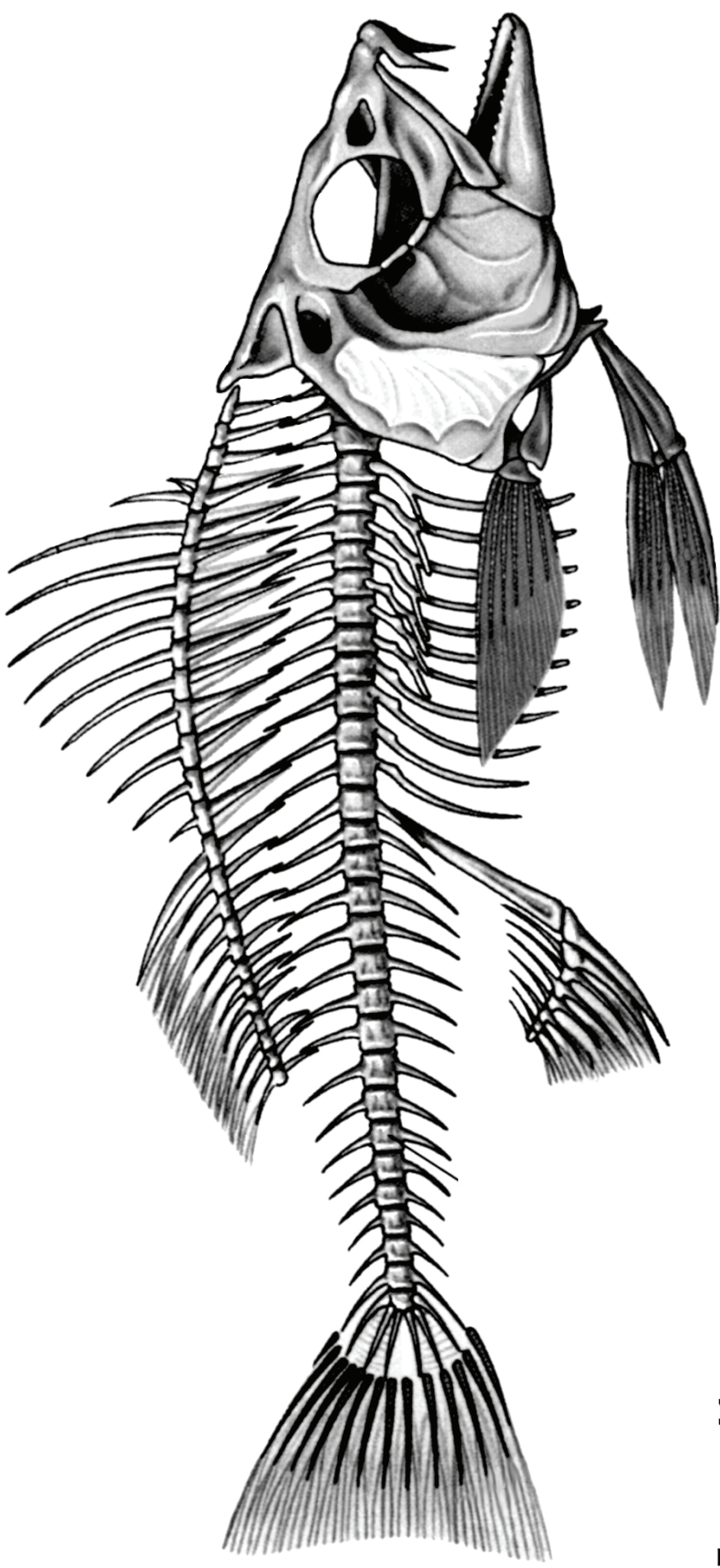


FIGURE 41 . Axial Skeleton of a modern bony fish (*Perca*). The chain of vertebrae comprising the vertebral column is differentiated into two distinct regions: the trunk region bears accessory processes on the centrum for the attachment of ribs whereas the caudal region is limited to neural and hemal spines.

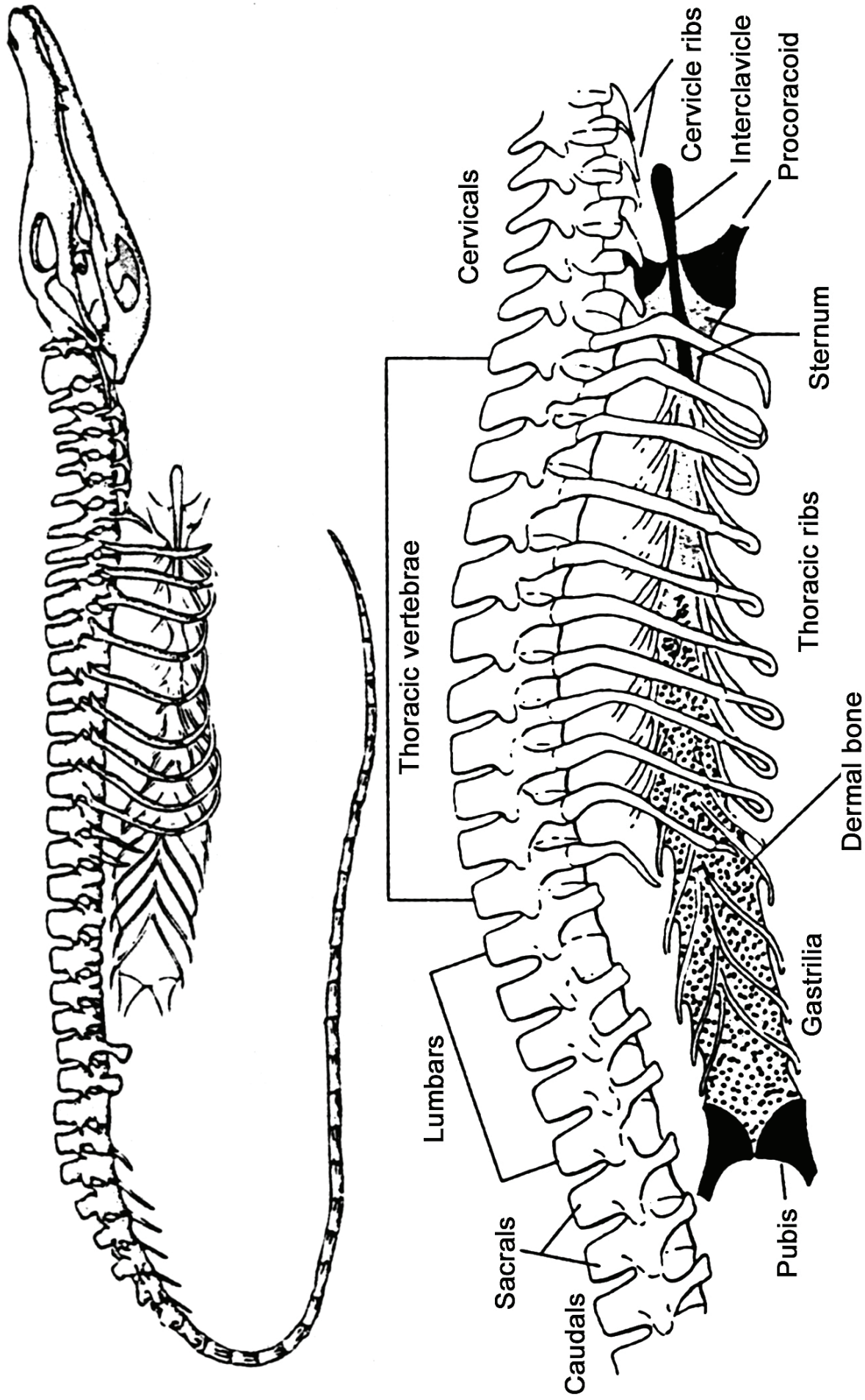


FIGURE 42. General regions of the axial skeleton in an alligator. The vertebral column of amniotes is differentiated into five distinct regions (cervical, thoracic, lumbar, sacral, and caudal).

